Microscopic study of antiferromagnetic ground state and possible high-field ordered state in $CeOs_4Sb_{12}$ using muon spin rotation and relaxation

T. U. Ito,[1] W. Higemoto,[1] K. Ohishi,[2] K. Satoh,[3] Y. Aoki,[4] S. Toda,[4] D. Kikuchi,[4] H. Sato,[4] and C. Baines[5]
[1]*Advanced Science Research Center, Japan Atomic Energy Agency, Tokai, Ibaraki 319-1195, Japan*
[2]*Advanced Meson Science Laboratory, RIKEN, Wako 351-0198, Japan*
[3]*Graduate School of Science and Engineering, Saitama University, Saitama, Saitama 338-8570, Japan*
[4]*Department of Physics, Tokyo Metropolitan University, Hachioji, Tokyo 192-0397, Japan*
[5]*Paul Scherrer Institute, CH 5232 Villigen PSI, Switzerland*
(Received 11 June 2009; revised manuscript received 28 May 2010; published 19 July 2010)

An antiferromagnetic (AFM) ground state and a possible high-field ordered state in magnetic fields $H > 1$ T of a filled-skutterudite compound $CeOs_4Sb_{12}$ were investigated by the muon spin rotation and relaxation method. In a zero applied field, a spontaneous local field due to the weak AFM ordering was observed below ~1.6 K. The magnetic volume fraction gradually increases below 1.6 K with decreasing temperature, suggesting that this phase is sensitive to sample quality. The magnitude of the ordered dipole moment in the AFM state was estimated to be in the range of 0.11–0.17 μ_B/Ce at 0.1 K. In a field of 2 T applied along the [001] direction, clear anomalies in the muon Knight shift and linewidth were observed at ~1.5 K, consistent with the phase-transition scenario into the high-field ordered state suggested from specific-heat, resistivity, elastic, and NMR anomalies. The possibility of multipole ordering in the high-field phase was discussed.

DOI: 10.1103/PhysRevB.82.014420 PACS number(s): 75.30.Kz, 71.27.+a, 76.75.+i

I. INTRODUCTION

A filled-skutterudite structure leads to a great variety of physical properties depending on the combination of constituent elements. Many filled-skutterudite compounds have been synthesized and several novel phenomena related to the unique crystal structure have been reported.[1–6] Among them, a series of cerium-based compounds CeT_4X_{12} (T: Fe, Ru, and Os, X: P, As, and Sb) is characterized by the hybridization gap caused by mixing between $4f$ electrons and conduction electrons.[7] The main conduction band is constructed by p orbitals of pnictogen atoms surrounding the Ce ion and a large coordination number of the pnictogen atoms results in strong p-f hybridization.[8]

$CeOs_4Sb_{12}$ is expected to be metallic from trends in the energy gap in the CeT_4X_{12} series as a function of the lattice constant.[7] In fact, a marked increase in resistivity was observed below 50 K in a zero applied field (ZF).[7,9] Excitations of tens of millielectron volt were detected by optical conductivity and inelastic neutron-scattering measurements at low temperatures, indicating the formation of a hybridization gap.[10,11] On the other hand, the electronic specific-heat coefficient $\gamma = 92-180$ mJ/K^2 mol (Refs. 9 and 12) suggests a heavy-fermion behavior at low temperatures. Recently, an electronic structure near the Fermi energy was studied in detail by photoemission spectroscopy and a model to explain these contradictory features was proposed[13] on the basis of symmetry-dependent hybridization.[8]

Another interesting feature of $CeOs_4Sb_{12}$ is an anomalous phase diagram of the low-temperature ordered state. Specific heat shows a small jump at ~0.9 K in ZF and a magnetic entropy ~$0.05R$ ln 2 (Ref. 12) is released. An increase in the NQR linewidth and suppression of the nuclear-spin-lattice relaxation rate T_1^{-1} were detected by ^{123}Sb-NQR. These were ascribed to a spin-density wave (SDW) or charge-density wave transition.[14] Finally, an antiferromagnetic (AFM) reflection with a wave vector $\boldsymbol{q}=(100)$ was observed by neutron diffraction, providing evidence for spontaneous AFM ordering.[15] The wave vector implies that the Fermi-surface instability of the filled skutterudite with a nesting vector $\boldsymbol{q}=(100)$ is closely related to the ground state of $CeOs_4Sb_{12}$.[8] The magnitude of the ordered dipole moment was estimated to be 0.07(2) μ_B/Ce from neutron-diffraction intensity.[16] The AFM reflection intensity shows a gradual increase below 1.6 K, which is considerably higher than the Néel temperature T_N determined from the specific-heat anomaly. This behavior was ascribed to the distribution of T_N owing to the inhomogeneity of samples.

The phase-transition temperature determined from specific-heat and resistivity anomalies is gradually enhanced with increasing magnetic field H above ~1 T and exhibits a reentrant behavior above ~7 T.[7,12] The disappearance of the AFM reflection in $\mu_0 H > 1$ T (Ref. 16) suggests a different order parameter above ~1 T from that in low magnetic fields. A ^{121}Sb nuclear-spin-lattice relaxation rate divided by temperature $1/(T_1T)$ exhibits a significant reduction below the phase-transition temperature T^* of the possible high-field phase in $\mu_0 H > 1$ T.[17] Namiki *et al.* mentioned the possibility of antiferroquadrupole (AFQ) ordering based on the resemblance of the characteristic phase diagram to that of typical AFQ ordering.[18–20] However, a magnetic entropy release, ~$0.06R$ ln 2 at 4 T,[12] below T^* is extremely small in comparison with that of the usual AFQ ordering. Moreover, specific-heat, resistivity, elastic constant, and the $1/(T_1T)$ anomalies at T^* become less distinctive with increasing magnetic field.[7,12,17,21] Thus, further investigations by means of microscopic probes are required to elucidate the nature of the unusual state at low temperatures.

In this paper, we report on ZF, longitudinal-field (LF), and transverse-field (TF) positive muon spin rotation and relaxation (μSR) measurements in single-crystalline $CeOs_4Sb_{12}$, in order to investigate the AFM ground state and the possible

ordered state in high magnetic fields from a microscopic point of view. μSR is highly sensitive to local magnetic fields at interstitial sites where implanted muons are localized. The local magnetic state of the AFM ground state was studied by ZF-μSR and LF-μSR with randomly oriented single crystals and TF-μSR with aligned single crystals in TF of 0.02 T applied along the [001] direction. We also investigated the possible high-field ordered state using the TF-μSR method in TF of 2 T applied along the [001] direction. Our results clearly demonstrate an intrinsic magnetic ordering with a small ordered dipole moment (0.11–0.17 μ_B/Ce) in the low-field phase and are consistent with the other experimental results in $\mu_0 H > 1$ T which suggest the existence of the high-field phase.

II. EXPERIMENTAL RESULTS

Single-crystalline samples of $CeOs_4Sb_{12}$ were prepared using the Sb-flux method. ZF- and LF-μSR measurements were carried out below 3 K down to 0.1 K at the πM3 beamline, PSI, Switzerland, and below 100 K down to 10.8 K at the D1 area, J-PARC MUSE, Japan, in order to investigate the AFM ground state. At J-PARC MUSE, a pulsed muon beam with a double-pulse structure at an interval of 0.60 μs is delivered to the experimental area. Single-crystalline samples were randomly oriented and glued with Apiezon N grease on the silver cold finger of a ^{3}He-^{4}He dilution refrigerator at PSI and of a ^{4}He gas flow cryostat at J-PARC MUSE. Spin-polarized positive muons were implanted into the samples and the asymmetry of positron emission owing to μ-e decay was recorded as a function of time t. ZF- and LF-μSR data $AP(t)$ were obtained, with A representing full asymmetry and $P(t)$ the projection of the muon spin-polarization vector onto an axis of positron detectors.

TF-μSR measurements below 3.0 K down to 0.1 K were performed at the M15 beamline, TRIUMF, Canada. Single crystals were glued with GE varnish on the (111) plane of a single-crystalline GaAs wafer,[22] which was mounted on the silver cold finger of the ^{3}He-^{4}He dilution refrigerator with Apiezon N grease. Positive muons were implanted into the samples with the initial spin-polarization direction perpendicular to the [001] direction and TF was applied along the [001] direction. The TF-μSR data were taken at magnetic fields of 0.02 and 2 T to investigate the AFM ground state and the possible high-field ordered state. We describe the results below.

A. AFM ground state

1. ZF and LF μSR

Typical ZF-μSR spectra below 3.0 K are shown in Fig. 1. The background signal from the silver cold finger has been subtracted. In the paramagnetic state, nearly temperature-independent relaxation was observed, primarily due to the nuclear dipole moment of ^{121}Sb and ^{123}Sb. The ZF spectra in the paramagnetic state can be expressed by the following function:

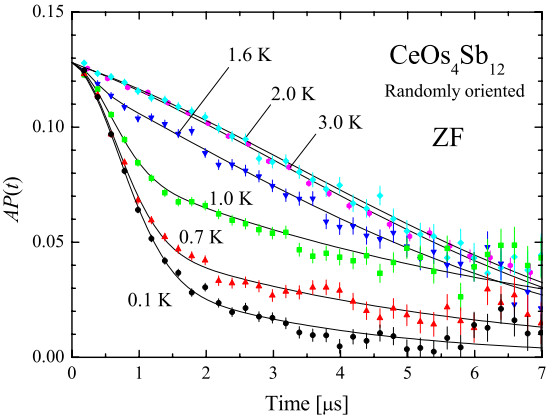

FIG. 1. (Color online) ZF-μSR spectra at several temperatures. The background signal has been subtracted.

$$AP(t) = Ae^{-\lambda t} G_{KT}(t), \tag{1}$$

$$G_{KT}(t) = \frac{1}{3} + \frac{2}{3}(1 - \Delta^2 t^2)\exp\left(-\frac{1}{2}\Delta^2 t^2\right), \tag{2}$$

where A is the total asymmetry of the signal from the samples, Δ and λ are relaxation rates, $G_{KT}(t)$ is the static ZF Kubo-Toyabe function, which suitably describes muon spin relaxation in dense nuclear spin systems.[23] The relaxation rates Δ, λ obtained for ZF data above 2 K using Eq. (1) are shown in Fig. 2. The double-pulse structure is taken into account to analyze the data above 10.8 K obtained at J-PARC MUSE. Details of data analysis for the double-pulsed μSR are given in the Appendix. Δ, which dominates the trend of $AP(t)$, is almost constant between 2 and 100 K, while λ exhibits a slight increase with decreasing temperature. This behavior in λ is presumably related to f-electron dynamics.

Below 1.6 K, the shape of the ZF spectra suddenly varies from that in the paramagnetic state. The Gaussian-shaped fast relaxation component appears and the fractional weight of this signal gradually increases with decreasing temperature. At our lowest temperature of 0.1 K, the ZF spectrum consists of the fast relaxation component and an exponential-shaped slow relaxation component with relative amplitude $\sim 2:1$. These facts suggest that the magnetic volume fraction

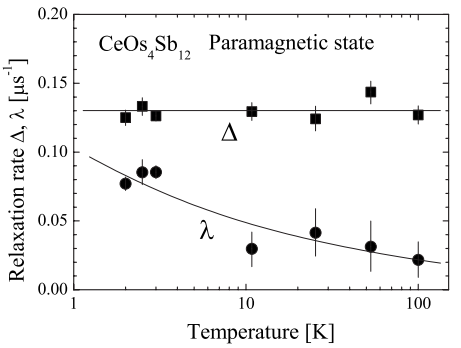

FIG. 2. The temperature dependence of ZF relaxation rates Δ (solid square) and λ (solid circle) in the paramagnetic state. The solid lines are guides for the eyes.

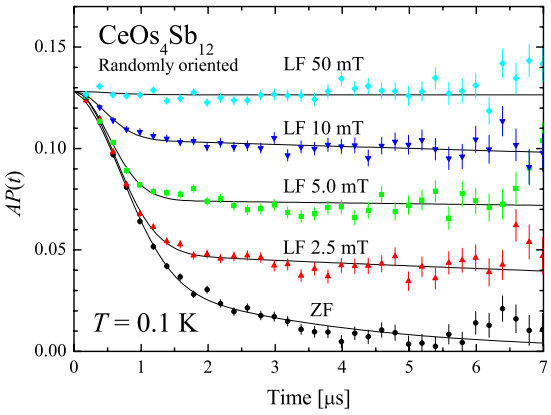

FIG. 3. (Color online) LF-μSR spectra at 0.1 K at several LFs. The background signal has been subtracted. The solid curves are the best fits with Eq. (3).

gradually increases below 1.6 K with decreasing temperature and almost the whole volume of the samples is in the AFM state at 0.1 K. It is difficult to extract temperature variation in relaxation parameters below 1.6 K from the ZF spectra since magnetic and paramagnetic parts in the slow relaxation component cannot be distinguished. Such analysis will be carried out later using low-TF data.

Figure 3 shows $AP(t)$ in several LFs at 0.1 K. The background signal from the silver cold finger has been subtracted. The fast relaxation component in ZF gradually fades away with increasing LF H_{LF} and is replaced with a nearly constant component. This behavior is evidence for a static local field B_{loc} at the muon site. All the ZF and LF spectra can be suitably explained by the following function:

$$AP(t) = A_1 e^{-\sigma^2 t^2} + A_2 e^{-\lambda t}, \tag{3}$$

where A_1 and A_2 are partial asymmetries of the fast and slow relaxation components, respectively, and σ and λ are relaxation rates. The LF dependence of the relative amplitude of the nearly constant component A_2/A shown in Fig. 4 is connected with the magnitude of the local field. When B_{loc} assumes a unique value with isotropic distribution, the LF dependence of A_2/A is explained by the following function:

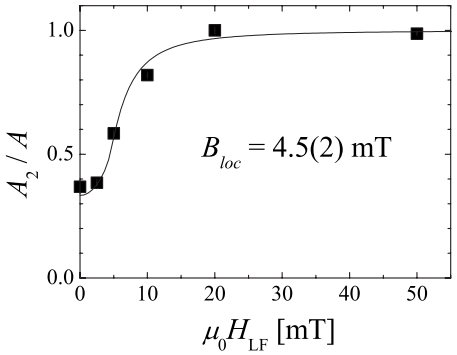

FIG. 4. The LF dependence of A_2/A at 0.1 K. The solid line is the best fit with Eq. (4).

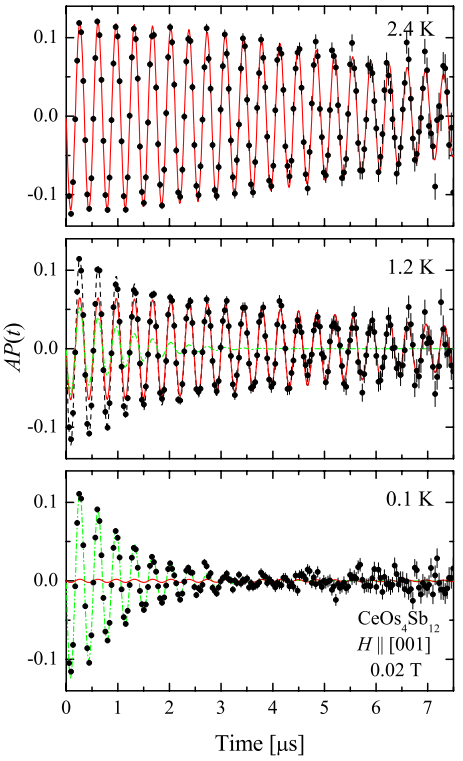

FIG. 5. (Color online) TF-μSR spectra at several temperatures. The background signal has been subtracted. The broken curves (black) are the best fits with Eq. (6). Contributions from the magnetic and paramagnetic component are shown by the dashed curves (green) and solid curves (red) drawn over the broken curves, respectively.

$$\frac{A_2}{A} = \frac{3}{4} - \frac{1}{4x^2} + \frac{(x^2-1)^2}{16x^3}\log\frac{(x+1)^2}{(x-1)^2}, \tag{4}$$

$$x = \frac{\mu_0 H_{\mathrm{LF}}}{B_{loc}}. \tag{5}$$

We adopted this model to analyze $A_2/A(H_{\mathrm{LF}})$ and a satisfactory fit was obtained, as shown in Fig. 4. From this analysis, the magnitude of the local field at 0.1 K was estimated to be 4.5(2) mT.

2. TF μSR

Typical TF-μSR spectra in a field of 0.02 T are shown in Fig. 5. The background signal from the diamagnetic muonium in GaAs has been subtracted.[24] In the paramagnetic state above 2 K, nearly temperature-independent relaxation, mainly due to the nuclear dipole moment of ^{121}Sb and ^{123}Sb, was observed. A fast relaxation component ascribed to the weak AFM ordering emerges below $\sim$1.6 K, the fractional weight of which, p_m, increases with decreasing temperature. The relaxation rate of the remaining slow relaxation component is comparable in magnitude to that in the paramagnetic state, suggesting that part of the samples remains paramagnetic below $\sim$1.6 K. These facts again imply some distribution of T_{N} in our samples.

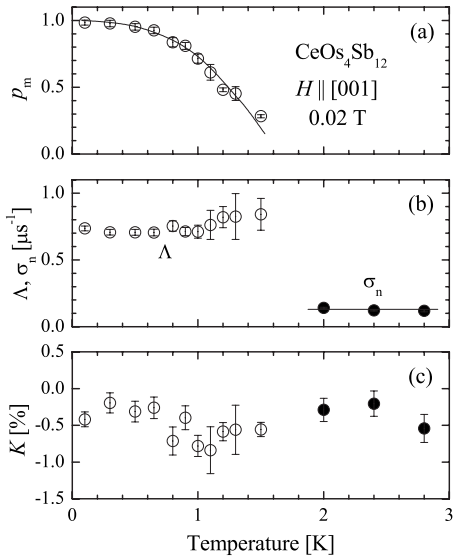

FIG. 6. The temperature dependence of (a) the magnetic volume fraction p_m, (b) the relaxation rate Λ and σ_n, and (c) the muon Knight shift K deduced from the TF-μSR spectra in a field of 0.02 T using χ^2-minimization fits with Eq. (6). The solid lines are guides for the eyes.

We use the following function to analyze data based on this physical picture:

$$AP(t) = A[p_m e^{-(\Lambda t)^\beta - \sigma_n^2 t^2} + (1 - p_m) e^{-\sigma_n^2 t^2}] \times \cos(\omega t + \phi), \tag{6}$$

where A is the total asymmetry of the signal from the samples, β is the exponent of the relaxation function for the magnetic component, ω is the angular frequency, ϕ is the initial phase, and Λ and σ_n are relaxation rates attributed to the magnetism of electron and nucleus, respectively. Here we ignore a possible difference in angular frequency between the magnetic and paramagnetic components, which is not noticeable in the present case (as shown later).

For analysis of data above 2 K in the paramagnetic state, χ^2 minimization fits were carried out on condition of p_m=0. The relaxation rate σ_n and the muon Knight shift $K \equiv (\omega - \omega_0)/\omega_0$ were obtained from the fits, as shown with the solid circles in Figs. 6(b) and 6(c), where ω_0 is the zero-shift angular frequency. We regard an angular frequency of the background signal from the diamagnetic muonium in GaAs as ω_0, the Knight shift of which is within ~10 ppm.[25] The relaxation rate σ_n was set to be 0.122 μs^{-1} through fits of the data below 2 K, which is an average of σ_n above 2 K. The value of β was determined to be 1.31 from a fit of the lowest temperature data and was fixed through the other fits. Satisfactory fits were obtained with the reduced χ^2 ranging from 0.93 to 1.05. It should be noted that a single-component fit with p_m=1 results in nearly twice as large χ^2 as that with our two-component model. The best fits are indicated by broken curves (black) in Fig. 5 with contributions from the magnetic and paramagnetic component expressed by dashed curves (green) and solid curves (red), respectively. All the parameters extracted by the fits are shown in Fig. 6 with the open circles as functions of temperature. The magnetic volume fraction p_m shows a gradual increase below ~1.6 K. This temperature is rather higher than T_N=0.9 K determined from the specific-heat anomaly but coincides with the temperature at which the AFM reflection intensity starts to rise with decreasing temperature. The relaxation rate Λ ascribed to the ordered dipole moment is 0.74(2) μs^{-1} at 0.1 K. This is only about six times larger than the σ_n attributed to the nuclear dipole moment, suggesting that the ordered dipole moment is considerably small in magnitude. It should be noted that no significant change in K was detected from 2.8 K down to 0.1 K. This is probably responsible for the insufficient experimental accuracy with regard to ω in such a low field.

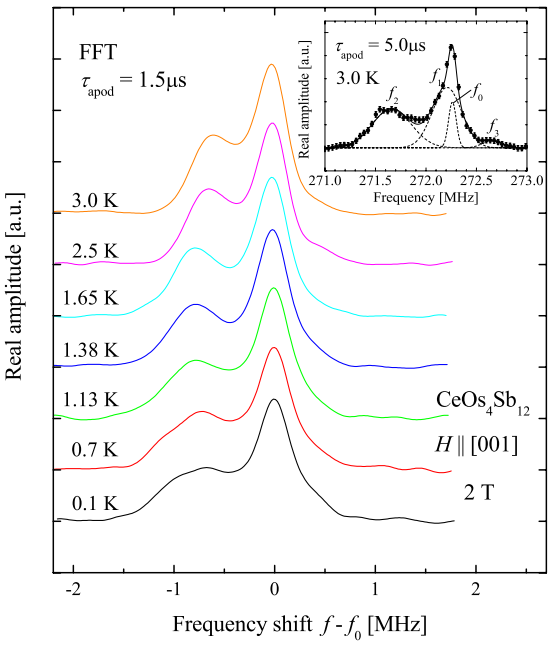

FIG. 7. (Color online) FFT spectra of the TF-μSR signals recorded in a field of 2 T at several temperatures in the form of frequency shift $f-f_0$. The apodization constant τ_{apod}=1.5 μs was set to suppress unessential oscillations in the spectra. The inset shows the FFT spectrum at 3.0 K transformed on condition of τ_{apod}=5.0 μs. The solid curve indicates the best fit with Eq. (7) converted into the frequency space. The dashed curves express contributions from each component.

B. Possible high-field ordered state

The TF-μSR spectra in a field of 2 T exhibit a clear beat structure, indicating that the spectra consist of a sum of several oscillatory signals with different frequencies. Fast Fourier-transform (FFT) spectra of the TF-μSR signals are shown in Fig. 7 in the form of a frequency shift $f-f_0$, where f_0 is the zero-shift frequency. A Gaussian apodization function, $\exp(-t^2/2\tau_{apod}^2)$, was multiplied on $AP(t)$ before the FFT to suppress unessential oscillations in the FFT spectra. The apodization constant τ_{apod}=1.5 μs was chosen. A two-peak structure is clearly seen in the frequency domain, both in the paramagnetic and the possible high-field ordered state. This indicates that a ferromagnetic (FM) component of field-

induced (FI) dipole moment dominates the local field at the muon site in the possible high-field ordered state as well as in the paramagnetic state. In order to examine the peak structure in detail, a FFT spectrum at 3.0 K with a larger τ_{apod} of 5.0 μs is shown in the inset of Fig. 7. The higher-frequency peak has an asymmetric feature and can be decomposed to two signals: a sharp background signal from the diamagnetic muonium in GaAs (f_0) and a broad signal which shows small negative shift (f_1). On the other hand, the lower-frequency peak (f_2) can be regarded as a single Gaussian. In addition, a signal of minute amplitude (f_3) is found on the high-frequency side. Thus, we analyze the TF-μSR spectra in a field of 2 T using the following function:

$$AP(t) = \sum_{i=1}^{3} A_i e^{-\sigma_i^2 t^2} \cos(\omega_i t + \phi) + A_0 e^{-\sigma_0^2 t^2} \cos(\omega_0 t + \phi), \tag{7}$$

where A_i, σ_i, and ω_i are the partial asymmetry, relaxation rate, and angular frequency of the signal f_i, respectively. The last term represents the background signal from the diamagnetic muonium in GaAs.[26] In a high magnetic field of 2 T, the FM component of the FI dipole moment dominates over σ_i as well as $\delta\omega_i \equiv \omega_i - \omega_0$, and it is difficult to distinguish a contribution from the nuclear dipole field to σ_i. Also note that the splitting of the signal in this condition is not due to the phase separation discussed in the AFM ground state, but due to symmetry lowering caused by the FI dipole moment, since that was observed in the paramagnetic state. The partial asymmetries, $(A_1, A_2, A_3, A_0) = (0.077, 0.067, 0.004, 0.016)$, were determined by the fit of the data at 3.0 K and set to be constant through the other fits. Since the intensity of the signal f_3 is one order of magnitude smaller than that of the other signals, f_3 can probably be ascribed to a misaligned portion of the samples. We will not discuss this signal further since the statistics of the data are not high enough to discuss the parameters of such a small signal.

Satisfactory fits with the reduced χ^2 ranging from 0.94 to 1.14 were obtained using Eq. (7). Note that the assumption of the phase separation is not necessary in this case in order to receive a good reduced χ^2 unlike the AFM ground state. The muon Knight shift of the signal f_i was derived from the following relation: $K_i = (\omega_i - \omega_0)/\omega_0$. The Knight shifts of the two main signals, K_1 and K_2, are plotted in Fig. 8. These show a clear anomaly at $\sim$1.5 K, which roughly agrees with T^* determined from the specific-heat and resistivity anomalies.[7,12] Figure 9 shows the temperature dependence of σ_1 and σ_2. A significant increase is found below T^* in both σ_1 and σ_2. These results are consistent with the phase-transition scenario in high magnetic fields $H > 1$ T. It should be noted that our microscopic and static data are complementary to dynamical information provided by T_1^{-1} measurements of ^{121}Sb NMR.[17]

III. DISCUSSION

In this section we describe the implications of the ZF-, LF-, and TF-μSR results in the AFM ground state at 0.02 T and the TF-μSR results in the possible high-field ordered state at 2 T, respectively.

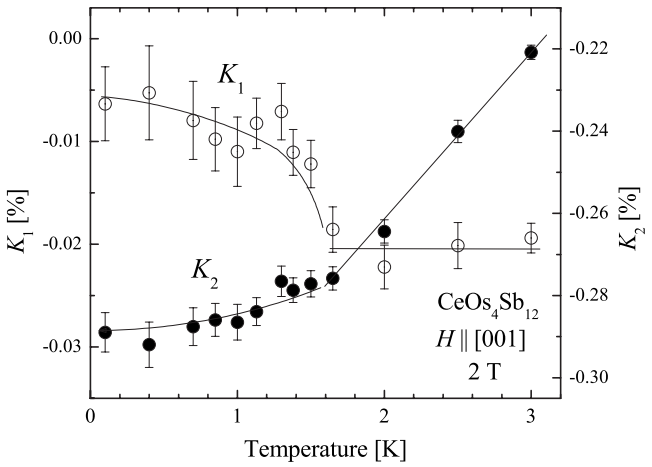

FIG. 8. The temperature dependence of K_1 (open circle) and K_2 (solid circle) deduced from the TF-μSR spectra in a field of 2 T applied along the [001] direction with Eq. (7). The solid lines are guides for the eyes.

A. AFM ground state

We demonstrated in Sec. II A that relaxation attributed to the magnetism of electrons develops below $\sim$1.6 K. The static nature of the local field at the muon site was manifested by LF-μSR. Thus, we conclude that a spontaneous magnetic ordering occurs below $\sim$1.6 K, which is consistent with the AFM reflection observed by neutron diffraction.[16] The magnitude of the local field B_{loc} was estimated to be 4.5(2) mT at 0.1 K. On the other hand, no clear muon spin precession owing to the spontaneous field was found in the μSR spectra, despite the simple wave vector $\boldsymbol{q} = (100)$ of the AFM reflection, suggesting inhomogeneity of the ordered state. In contrast, a distinct muon spin precession was observed by ZF-μSR measurements in the weak FM ordering phase of isomorphic $SmOs_4Sb_{12}$.[27] This is probably related to the distribution of T_N suggested by the gradual change in p_m, as shown in Fig. 6(a). Our result indicates possible spatial

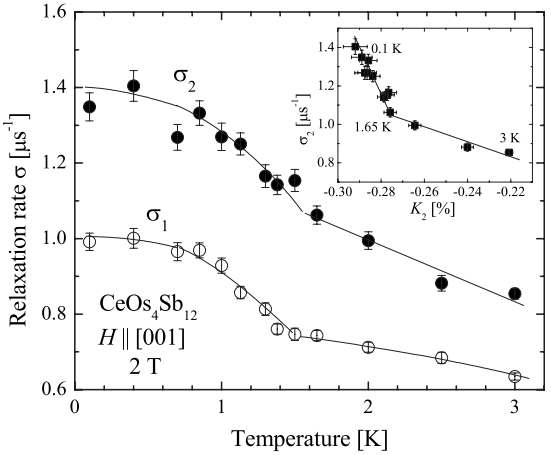

FIG. 9. The temperature dependence of σ_1 (open circle) and σ_2 (solid circle) extracted from the TF-μSR spectra in a field of 2 T applied along the [001] direction with Eq. (7). The inset is the σ_2 versus K_2 plot. The solid lines are guides for the eyes.

distribution of sample quality which influences low-temperature phases, at least the AFM ground state in low fields. The low-field region of the phase diagram based on macroscopic measurements should be carefully reexamined.

In order to evaluate the magnitude of the ordered dipole moment, the distance between the muon and Ce ions must be given. Candidates for the muon site in isomorphic $RE\mathrm{Os_4Sb_{12}}$ (*RE*: rare-earth) systems have been discussed by Aoki *et al.*[28] in $\mathrm{PrOs_4Sb_{12}}$ and $\mathrm{SmOs_4Sb_{12}}$,[27] and by Shu *et al.*[29] in $\mathrm{Pr_{1-x}La_xOs_4Sb_{12}}$. They suggested the most probable $(0,\frac{1}{2},0.15)$ site (12*e* in the Wyckoff notation) in the filled-skutterudite structure based on the magnitude of the nuclear dipole field. In our case, the experimental value of $\Delta \sim 0.13\ \mu\mathrm{s}^{-1}$ corresponds to a field spread $\sim 1.5\times 10^{-4}$ T at the muon site, due to the nuclear dipole contribution. This is close to a calculated value of 2.0×10^{-4} T for the 12*e* site. We therefore evaluate the magnitude of the ordered dipole moment assuming this muon site. A classical dipole field at the muon site in the AFM state was calculated on the assumption that the AFM wave vector is $\boldsymbol{q}=(001)$ (Ref. 16) and the direction of the ordered dipole moment is parallel to any one of the symmetrical axes $\langle 001\rangle$, $\langle 110\rangle$, and $\langle 111\rangle$. From $B_{loc}=4.5(2)$ mT at 0.1 K, the magnitude of the ordered dipole moment was estimated to be in the range of $0.11-0.17\ \mu_B/\mathrm{Ce}$. This is somewhat larger than the value obtained from the neutron-diffraction data, $0.07(2)\ \mu_B$.[16] Our results are consistent with the SDW-like weak AFM ordering scenario, suggesting strong itinerancy of 4*f* electrons in low fields caused by *p*-*f* hybridization.

B. Possible high-field ordered state

The microscopic support of the phase-transition scenario into the high-field ordered state was provided by our TF-μSR measurements in a field of 2 T based on the anomalies in static physical quantities, K_i and σ_i. These findings are complementary to the dynamical information provided by the T_1^{-1} measurements of ^{121}Sb NMR.[17]

Supposing that the phase transition really occurs at T^*, the order parameter in the high-field phase should be different from that in the low-field phase, since the AFM reflection intensity detected by neutron diffraction decreases with increasing field and disappears above ~ 1 T.[16] The FM component of the FI dipole moment is dominant to the local field at the muon site in this state, as was mentioned in Sec. II B. The anomaly in K_i at around T^*, as shown in Fig. 8, indicates modulation of the FI dipole moment in the ordered state. The linewidth, which is proportional to σ_i, increases significantly below T^* as expressed in Figs. 7 and 9. The anomaly in σ_2 is emphasized in the σ_2 versus K_2 plot shown in the inset of Fig. 9, where linear behavior above 1.6 K suggests that σ_2 in the paramagnetic state is primarily due to field distributions originating from inhomogeneity of K_i. The change in the slope at around T^* implies that additional field distributions develop in the ordered state. We decompose the relaxation rate as $\sigma=(\sigma_n^2+\sigma_{\delta K}^2+\sigma_{order}^2)^{1/2}$, where temperature-independent σ_n is caused by the nuclear dipole field distributions and/or inhomogeneity of the applied field, $\sigma_{\delta K}(\propto K)$ originates from the inhomogeneity of K, and σ_{order} is the additional relaxation rate which develops in the ordered state. The magnitude of σ_{order} at 0.1 K is roughly estimated to be 0.7 $\mu\mathrm{s}^{-1}$ for σ_1 from the temperature dependence of σ_1, 0.8 $\mu\mathrm{s}^{-1}$ for σ_2 from the σ_2-K_2 relation. These values are comparable in magnitude with the TF relaxation rate Λ in a field of 0.02 T in the small moment AFM state, as shown in Fig. 6. If the order parameter of the high-field phase is nonmagnetic, the rise in σ_{order} is presumably ascribed to the appearance of an AFM component in the FI dipole moment, corresponding to spatial modulation of the nonmagnetic order parameter[30] and/or distributions of the FI moment direction due to the formation of ordered domains. On the other hand, an ordered magnetic multipole moment can be a primary source of σ_{order} when the order parameter is magnetic. Unfortunately, we cannot distinguish these possibilities from our μSR data alone.

FM or AFM dipole ordering is unlikely from the *H*-*T* phase diagram, where the phase boundary $T^*(H)$ of the high-field ordered state exhibits $dT^*/dH>0$ behavior in low fields and reentrant behavior above ~ 7 T.[7,12] Such a phase diagram is found in AFQ ordering in $\mathrm{CeB_6}$,[18] $\mathrm{PrPb_3}$,[19] and TmTe,[20] and possible octupole ordering in $\mathrm{SmRu_4P_{12}}$ (Ref. 5) (only the $dT^*/dH>0$ behavior was confirmed), suggesting a possibility of high-order multipole ordering in $\mathrm{CeOs_4Sb_{12}}$. The AFQ ordering seems incompatible with the elastic constant in $H\|[001]$, which shows no clear anomaly at T^* in high magnetic fields.[21] Meanwhile, a recent angle-resolved specific-heat study revealed that the specific-heat anomaly at T^* is markedly suppressed in the case of $H\|[001]$, in comparison with other field directions.[31] Therefore, elastic constant measurements in magnetic fields applied along the other field directions are necessary in order to discuss quadrupole interactions in high magnetic fields. Another possibility, a magnetic octupole ordering, is not inconsistent with our results, producing a local field at the muon site which results in the increase in σ_{order}.[32–35] In any case, multipole degrees of freedom which belong to the Γ_{67} quartet are required for the high-order multipole ordering scenario, although no clear crystal-field excitation has been detected.[36] The high-field ordered state in $\mathrm{CeOs_4Sb_{12}}$ might be a new class of multipole ordering in *f*-electron systems with itinerant character. In order to identify the order parameter in the high-field phase, detailed field-angle-resolved measurements are required.

IV. CONCLUSIONS

The AFM ground state and the possible high-field ordered state in $H>1$ T of the filled-skutterudite compound $\mathrm{CeOs_4Sb_{12}}$ were investigated by means of the μSR method. In ZF, a spontaneous local field due to the weak AFM ordering was observed below ~ 1.6 K. The magnetic volume fraction gradually increases below 1.6 K with decreasing temperature, suggesting that this phase is sensitive to sample quality. Supposing that the AFM wave vector is $\boldsymbol{q}=(001)$ and the direction of the ordered dipole moment is parallel to any one of the symmetrical axes $\langle 001\rangle$, $\langle 110\rangle$, and $\langle 111\rangle$, the magnitude of the ordered dipole moment in the AFM state was estimated to be in the range of $0.11-0.17\ \mu_B/\mathrm{Ce}$. In a

field of 2 T applied along the [001] direction, clear anomalies in the muon Knight shift and linewidth were observed at ~1.5 K, consistent with the phase-transition scenario into the high-field ordered state suggested from specific-heat, resistivity, elastic, and NMR anomalies. The possibility of multipole ordering in the high-field phase was discussed on the basis of the *H-T* phase diagram, which is consistent with our observations.

ACKNOWLEDGMENTS

We thank TRIUMF, PSI, and J-PARC μSR groups for experimental assistance, as well as K. Kaneko, S. Kambe, Y. Tokunaga, H. Chudo, T. D. Matsuda, Y. Haga, and K. Shimomura for helpful discussions. This work was supported by Grant-in-Aids for Scientific Research on Priority Area "Skutterudite," and Innovative Area "Heavy Electron," from the Ministry of Education, Culture, Sports, Science and Technology, Japan, and the KEK-MSL Inter-University Program for Oversea Muon Facilities.

APPENDIX: ANALYSIS OF DOUBLE-PULSED μSR DATA AT J-PARC MUSE

The muon beam at J-PARC MUSE has a double-pulse structure which depends on a time structure of the primary proton beam. The interval of the double pulses δ at J-PARC MUSE is 0.60 μs. One must take into account the double-pulse structure in order to analyze the data obtained without a single-pulse extraction procedure using special devices.

Many muon spin relaxation theories have been developed to explain μSR spectra obtained by using continuous or single-pulsed muon beams. Thus, we here show the relation between the asymmetry of the conventional μSR, $A^0(t)$, and that of the double-pulsed μSR, $A^{DP}(t)$.

$A^0(t)$ can be extracted from the number of positron events detected by a forward counter placed upstream, $N_F^0(t) = N_F^0 e^{-t/\tau_\mu}[1+A^0(t)]$, and a backward counter positioned downstream, $N_B^0(t) = N_B^0 e^{-t/\tau_\mu}[1-A^0(t)]$, for the continuous or single-pulsed muon beam as follows:

$$A^0(t) = \frac{N_F^0(t) - \alpha N_B^0(t)}{N_F^0(t) - \alpha N_B^0(t)}, \tag{A1}$$

$$\alpha = N_F^0/N_B^0, \tag{A2}$$

where $\tau_\mu = 2.2$ μs is the muon lifetime.

The double-pulsed muon beam at J-PARC MUSE is composed of two single pulses with equal intensity at the interval δ. Therefore, $A^{DP}(t)$ is expressed as

$$A^{DP}(t) = \frac{N_F^0(t) + N_F^0(t+\delta) - \alpha[N_B^0(t) + N_B^0(t+\delta)]}{N_F^0(t) + N_F^0(t+\delta) + \alpha[N_B^0(t) + N_B^0(t+\delta)]} = \frac{A^0(t) + e^{-\delta/\tau_\mu} A^0(t+\delta)}{1 + e^{-\delta/\tau_\mu}}, \tag{A3}$$

where the origin of time is chosen at the center of the second pulse. Thus, the theoretical relaxation function $G^{DP}(t)$ to fit the double-pulsed μSR data is described as the same form using that for conventional μSR data $G^0(t)$, i.e.,

$$G^{DP}(t) = \frac{G^0(t) + e^{-\delta/\tau_\mu} G^0(t+\delta)}{1 + e^{-\delta/\tau_\mu}}. \tag{A4}$$

Note that the above discussion does not take account of the effect of pulse width. This should be treated carefully when the relaxation rate is comparable to the inverse of the pulse width.

[1] E. D. Bauer, N. A. Frederick, P.-C. Ho, V. S. Zapf, and M. B. Maple, Phys. Rev. B **65**, 100506(R) (2002).
[2] Y. Aoki, T. Namiki, S. Ohsaki, S. R. Saha, H. Sugawara, and H. Sato, J. Phys. Soc. Jpn. **71**, 2098 (2002).
[3] J. Kikuchi, M. Takigawa, H. Sugawara, and H. Sato, J. Phys. Soc. Jpn. **76**, 043705 (2007).
[4] K. Iwasa, L. Hao, K. Kuwahara, M. Kohgi, S. R. Saha, H. Sugawara, Y. Aoki, H. Sato, T. Tayama, and T. Sakakibara, Phys. Rev. B **72**, 024414 (2005).
[5] M. Yoshizawa, Y. Nakanishi, M. Oikawa, C. Sekine, I. Shirotani, S. R. Saha, H. Sugawara, and H. Sato, J. Phys. Soc. Jpn. **74**, 2141 (2005).
[6] S. Sanada, Y. Aoki, A. Tsuchiya, D. Kikuchi, H. Sugawara, and H. Sato, J. Phys. Soc. Jpn. **74**, 246 (2005).
[7] H. Sugawara, S. Osaki, M. Kobayashi, T. Namiki, S. R. Saha, Y. Aoki, and H. Sato, Phys. Rev. B **71**, 125127 (2005).
[8] H. Harima and K. Takegahara, J. Phys.: Condens. Matter **15**, S2081 (2003).
[9] E. D. Bauer, A. Ślebarski, E. J. Freeman, C. Sirvent, and M. B. Maple, J. Phys.: Condens. Matter **13**, 4495 (2001).
[10] D. T. Adroja, J. G. Park, E. A. Goremychkin, K. A. McEwen, N. Takeda, B. D. Rainford, K. S. Knight, J. W. Taylor, J. Park, H. C. Walker, R. Osborn, and P. S. Riseborough, Phys. Rev. B **75**, 014418 (2007).
[11] M. Matsunami, H. Okamura, T. Nanba, H. Sugawara, and H. Sato, J. Phys. Soc. Jpn. **72**, 2722 (2003).
[12] T. Namiki, Y. Aoki, H. Sugawara, and H. Sato, Acta Phys. Pol. B **34**, 1161 (2003).
[13] M. Matsunami, R. Eguchi, T. Kiss, K. Horiba, A. Chainani, M. Taguchi, K. Yamamoto, T. Togashi, S. Watanabe, X. Y. Wang, C. T. Chen, Y. Senba, H. Ohashi, H. Sugawara, H. Sato, H. Harima, and S. Shin, Phys. Rev. Lett. **102**, 036403 (2009).
[14] M. Yogi, H. Kotegawa, G. Q. Zheng, Y. Kitaoka, S. Ohsaki, H. Sugawara, and H. Sato, J. Phys. Soc. Jpn. **74**, 1950 (2005).
[15] C. P. Yang, H. Wang, J. F. Hu, K. Iwasa, M. Kohgi, H. Sugawara, and H. Sato, J. Phys. Chem. C **111**, 2391 (2007).
[16] K. Iwasa, S. Itobe, C. Yang, Y. Murakami, M. Kohgi, K. Kuwahara, H. Sugawara, H. Sato, N. Aso, T. Tayama, and T. Sakakibara, J. Phys. Soc. Jpn. **77**, Supplement A, 318 (2008).
[17] M. Yogi, H. Niki, M. Yashima, H. Mukuda, Y. Kitaoka, H. Sug-

awara, and H. Sato, J. Phys. Soc. Jpn. **78**, 053703 (2009).
[18] R. G. Goodrich, D. P. Young, D. Hall, L. Balicas, Z. Fisk, N. Harrison, J. Betts, A. Migliori, F. M. Woodward, and J. W. Lynn, Phys. Rev. B **69**, 054415 (2004).
[19] T. Tayama, T. Sakakibara, K. Kitami, M. Yokoyama, K. Tenya, H. Amitsuka, D. Aoki, Y. Ōnuki, and Z. Kletowski, J. Phys. Soc. Jpn. **70**, 248 (2001).
[20] T. Matsumura, S. Nakamura, T. Goto, H. Amitsuka, K. Matsuhira, T. Sakakibara, and T. Suzuki, J. Phys. Soc. Jpn. **67**, 612 (1998).
[21] Y. Nakanishi, T. Kumagai, M. Oikawa, T. Tanizawa, M. Yoshizawa, H. Sugawara, and H. Sato, Phys. Rev. B **75**, 134411 (2007).
[22] An undoped GaAs single crystal obtained from the MaTecK GmbH was used to reduce intensity of the zero-shift frequency signal, which is usually huge when samples are directly mounted on a silver sample holder.
[23] R. S. Hayano, Y. J. Uemura, J. Imazato, N. Nishida, T. Yamazaki, and R. Kubo, Phys. Rev. B **20**, 850 (1979).
[24] Muons implanted into the undoped GaAs wafer take the form of the T-center muonium (Mu_T), the bond-center muonium (Mu_{BC}), and the diamagnetic muonium. In low TF, signals from the Mu_T and Mu_{BC} disappear immediately due to the nuclear dipole field and/or the quantum diffusion of the muonium at low temperatures. These can be ignored in the present case while a signal from the diamagnetic muonium is an observable.
[25] K. L. Hoffman, K. H. Chow, R. F. Kiefl, B. Hitti, T. L. Estle, and R. L. Lichti, Physica B **326**, 175 (2003).
[26] In a high TF of 2 T applied along the $\langle 111 \rangle$ direction of the GaAs single crystal, the Mu_T signal is supposed to split into two components with frequencies in several gigahertz while four Mu_{BC} signals are expected to appear in the frequency space around a signal from the diamagnetic muonium at an interval of $\sim$50 MHz. However, the Mu_T and Mu_{BC} frequencies were not observed in our case, the asymmetry of which $\sim$0.1 was lost in the TF-μSR spectra. Thus, we ignore these signals and use Eq. (7) for analysis.
[27] Y. Aoki, W. Higemoto, Y. Tsunashima, Y. Yonezawa, K. H. Satoh, A. Koda, T. U. Ito, K. Ohishi, R. H. Heffner, D. Kikuchi, and H. Sato, Physica B **404**, 757 (2009).
[28] Y. Aoki, A. Tsuchiya, T. Kanayama, S. R. Saha, H. Sugawara, H. Sato, W. Higemoto, A. Koda, K. Ohishi, K. Nishiyama, and R. Kadono, Phys. Rev. Lett. **91**, 067003 (2003).
[29] L. Shu, D. E. MacLaughlin, Y. Aoki, Y. Tunashima, Y. Yonezawa, S. Sanada, D. Kikuchi, H. Sato, R. H. Heffner, W. Higemoto, K. Ohishi, T. U. Ito, O. O. Bernal, A. D. Hillier, R. Kadono, A. Koda, K. Ishida, H. Sugawara, N. A. Frederick, W. M. Yuhasz, T. A. Sayles, T. Yanagisawa, and M. B. Maple, Phys. Rev. B **76**, 014527 (2007).
[30] T. Onimaru, T. Sakakibara, N. Aso, H. Yoshizawa, H. S. Suzuki, and T. Takeuchi, Phys. Rev. Lett. **94**, 197201 (2005).
[31] Y. Aoki (unpublished).
[32] H. Takagiwa, K. Ohishi, J. Akimitsu, W. Higemoto, R. Kadono, M. Sera, and S. Kunii, J. Phys. Soc. Jpn. **71**, 31 (2002).
[33] W. Kopmann, F. J. Litterst, H. H. Klauß, M. Hillberg, W. Wagener, G. M. Kalvius, E. Schreier, F. J. Burghart, J. Rebizant, and G. H. Lander, J. Alloys Compd. **271-273**, 463 (1998).
[34] T. U. Ito, W. Higemoto, K. Ohishi, T. Fujimoto, R. H. Heffner, N. Nishida, K. Satoh, H. Sugawara, Y. Aoki, D. Kikuchi, and H. Sato, J. Phys. Soc. Jpn. **76**, 053707 (2007).
[35] T. U. Ito, W. Higemoto, K. Ohishi, R. H. Heffner, N. Nishida, K. Satoh, H. Sugawara, Y. Aoki, D. Kikuchi, and H. Sato, Physica B **404**, 761 (2009).
[36] C. P. Yang, M. Kohgi, K. Iwasa, H. Sugawara, and H. Sato, J. Phys. Soc. Jpn. **74**, 2862 (2005).